



THE STRUCTURE OF INFINITE PERIODIC AND CHAOTIC HUB CASCADES IN PHASE DIAGRAMS OF SIMPLE AUTONOMOUS FLOWS

JASON A. C. GALLAS
*Rechnergestützte Physik der Werkstoffe,
 ETH Hönggerberg HIF E12, Schafmattstrasse,
 CH-8093 Zurich, Switzerland*
*Instituto de Física,
 Universidade Federal do Rio Grande do Sul,
 91501-970 Porto Alegre, Brazil*

Received December 10, 2008; Revised April 22, 2009

This manuscript reports numerical investigations about the relative abundance and structure of chaotic phases in autonomous dissipative flows, i.e. in continuous-time dynamical systems described by sets of ordinary differential equations. In the first half, we consider flows containing “periodicity hubs”, which are remarkable points responsible for organizing the dynamics regularly over wide parameter regions around them. We describe *isolated hubs* found in two forms of Rössler’s equations and in Chua’s circuit, as well as surprising *infinite hub cascades* that we found in a polynomial chemical flow with a cubic nonlinearity. Hub cascades converge orderly to accumulation points lying on specific parameter paths. In sharp contrast with familiar phenomena associated with *unstable* orbits, hubs and infinite hub cascades always involve *stable* periodic and chaotic orbits which are, therefore, directly measurable in experiments. In the last part, we consider flows having no hubs but unusual phase diagrams: a cubic polynomial model containing *T*-points and wide regions of *dense chaos*, a nonpolynomial model of the Belousov–Zhabotinsky reaction and the Hindmarsh–Rose model of neuronal bursting, both having chaotic phases with “fountains of chaos”. The chaotic regions for the flows discussed here are different from what is known for discrete-time maps. This forcefully shows that knowledge about phase diagrams is quite fragmentary and that much work is still needed to classify and to understand them.

Keywords: Hubs and spirals; Rössler oscillators; chemical oscillators; Hindmarsh–Rose neuronal chaos; dense laser chaos; phase diagrams; global bifurcations; *T*-points; homoclinic orbits.

1. Introduction

Theoretical models of natural phenomena are routinely written nowadays in terms of the *æquatio differentialis* introduced by Leibniz in 1676 [Ince, 1926; Franceschetti, 1999]. The immense utility of differential equations in innumerable branches of natural sciences has been a subject which has received much attention and abundant illustration

for well over 300 years now [Segré, 2007]. In recent decades, discoveries concerning properties of differential equations arise almost exclusively from mathematical studies requiring sophisticated techniques and dealing mostly with unstable solutions and nondirectly measurable properties.

All this progress notwithstanding, the purpose of the present paper is to show that differential equations still harbor unanticipated regularities.

These novel regularities are not properties of isolated solutions. They may be recognized by contemplating the ordered way that large *families of solutions*, periodic or not, organize themselves collectively in parameter space. Extensive regions of regularities can be easily recognized in phase diagrams computed with enough resolution to display the chaotic regions and their inner structure. Regularities emerge in parameter space as a result of the self-organization of *stable* oscillations that, in principle, should not be too difficult to observe in the laboratory for a variety of popular oscillators across all disciplines of natural sciences.

Our main purpose here is to describe the regular self-organization observed while studying systematically an elementary problem always faced when simulating numerically natural phenomena modeled by differential equations: the necessity to discriminate and to classify periodic and aperiodic (chaotic) asymptotic steady states supported over extended parameter regions of interest.

The periodic or chaotic nature of steady states is traditionally determined on a case-by-case examination by fixing parameters and investigating the *phase space*, a space directly linked to the initial conditions. However, over the past few years, it has become increasingly easier to consider also the complementary *phase diagrams*, i.e. to exploit detailed *tomographic views* of the parameter space discriminating periodic from aperiodic oscillations over extended parameter regions [Bonatto *et al.*, 2005, 2008; Bonatto & Gallas, 2007, 2008a, 2008b; Freire *et al.*, 2008; Ramírez-Ávila & Gallas, 2008, 2009]. These works report phase diagrams for a number of prototypic oscillators like, for example, gas and semiconductor lasers, a resistive circuit involving a pair of diodes, variants of Chua’s circuit, atmospheric and chemical oscillators, and a few other oscillators. We briefly review what was found and present new results.

An unexpected feature found in the phase diagram of some oscillators is a focal point, a periodicity hub. Periodicity hubs were originally described for piecewise-linear electrical circuits [Bonatto & Gallas 2008; Ramírez-Ávila & Gallas 2008, 2009]. Figure 1 is a magnification of Fig. 2(b) of [Bonatto & Gallas, 2008] and shows a periodicity hub located at the focal point F . Apart from illustrating the organization around a hub, the main purpose of Fig. 1 is to define notation for two fundamental symmetry surfaces: S and h . The surface S divides phase diagrams into a *tame region*, here to the left

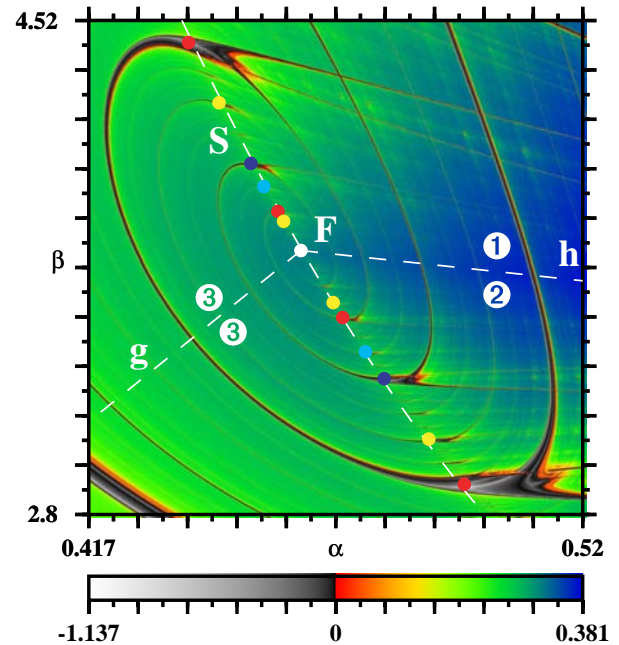


Fig. 1. The generic structure of parameter space around a focal hub in F . The symmetry surface S passes through F and through the colored dots which mark the main heads of the first few shrimps of an infinite sequence contained in the spirals curling up around F . Dots of identical colors lie on the same spiral. The surface S divides phase diagrams into a *tame region*, here to the left of S , and into a more *complex region*, to its right. The line h is the accumulation limit for pairs of legs emanating from every shrimp with main head centered in S , above and below F . The line h divides the complex region into two “mirror” sectors, indicated by the numbers 1 and 2 inside the circles. Hinged in F we draw a generic line g . Bifurcation diagrams along g display the same window structure as long as g remains on the left of S . This invariance implies the existence of a symmetrical third sector, indicated by the number 3 placed on both sides of g .

of S , and into a more *complex region*, to its right. The line h is the accumulation limit for pairs of legs emanating above and below from every shrimp centered along S . The line h divides the complex region into two “mirror” sectors, indicated by the numbers 1 and 2 inside circles. Microscopically, h is like a continuous string folded infinitely often to form a characteristic sheave of homoclinic loci, i.e. a continuous line emanating from a common saddle-focus equilibrium and containing an infinite number of bendings or, equivalently, folds, at regularly distributed points forming a mesh in the parameter plane. Except close to the folding, near a hub h looks locally like a “homoclinic doublet”, namely like a very narrowly-packed pair of curves running parallel until meeting each other to form the fold. At least numerically, periodicity hubs seem to be

located precisely at these bendings of the homoclinic locus. Attached to F we draw a generic line g that may be rotated up and down around F . We call it “generic” because bifurcation diagrams along g display the same window structure as long as g remains on the left of S . This invariance implies the existence of a self-symmetrical third sector, which we indicate by the number 3 placed on both sides of g . As corroborated by several of the figures below, the relative orientation of the symmetry surfaces S and h defines the generic parameter structuring observed around hubs.

As shown by Fig. 1, the organization around F is quite ordered and symmetric, with spiral nestings emanating from F or, equivalently, converging towards F . By suitably tuning parameters, periodic oscillations (obtained for parameters inside the dark spirals in Fig. 1) may have their waveform and periodicity changed continuously without bound and without ever crossing the vast surrounding chaotic phase (represented by the colors in the figure). The ordered organization around hubs is “auto-regulated” in the sense that it exists intrinsically, without need of any external force to drive it. Hubs and their selforganization are characteristic properties of certain flows. They are not difficult to detect numerically, despite the fact that there is no theoretical recipe to find them. Based on their relative abundance in numerical experiments, we expect hubs and their spirals to occur frequently in applications.

As mentioned above, the existence of *isolated* hubs was originally observed for piecewise-linear electrical circuits. A novelty reported here is that hubs appear not only isolated but in fact, quite surprisingly, form infinite hierarchical cascading which accumulate towards a *master hub* or, equivalently, arise from it. Such master hub acts like a sort of main source of an infinite hub network (see Fig. 7 below). The accumulation process underlying hub cascades leads to characteristic parameter paths, loci, with remarkably fertile structure. Every individual hub is the termination of a family of periodic orbits with waveforms evolving continuously and with period growing more and more, diverging without any bound when approaching the focal hub.

This paper is organized as follows. To setup the scenario, Sec. 2 describes phase diagrams with isolated hubs and infinite sequences of spirals attached to them. Section 3 presents a first key novel result, a dynamical system with *infinite sequences*

of hub cascades each one with infinite subcascades, *ad infinitum*, all accumulating in specific parameter points. Section 4 considers the so-called T -point in the phase diagram of a cubic polynomial model. Infinite sequences of spirals were previously observed in connection with such T -points [Glendinning & Sparrow, 1986], which are terminal points associated with particular heteroclinic loops in parameter space. The purpose of Sec. 4 is to present numerical evidence that the infinite sequences of *unstable* orbits associated with heteroclinic loops of a certain kind do not seem to be the cause of hubs. Section 5 presents our second key novel result, namely a flow containing a wide region of dense chaos, i.e. continuous chaos without periodic windows. Section 6 contains our conclusions.

Before proceeding, recall that there are no theoretical tools to predict the location and structure of chaotic regions or phases. Thus, one needs to resort to numerical simulations to find them, which is what we do here. In fact, the theory is in such a primitive stage that it is still very common to just state that “chaos is a property of nonlinear differential equations” instead of trying to move to the next logical level of addressing difficult and pressing questions: to find a theoretical way to predict when and where chaos should be expected in phase diagrams of physical systems governed by differential equations, and to anticipate the possible structure of such diagrams.

2. Isolated Hubs for Two Rössler’s Oscillators

This section reviews the phenomenology associated with hubs that are “macroscopically isolated” in parameter space, in the sense that no other hubs are detectable nearby. Instead of reviewing the original piecewise-linear circuits already mentioned, we consider here two normal forms of Rössler’s oscillators. These oscillators are of interest because their equations of motion have continuous derivatives but not the symmetries of the piecewise-linear circuits.

Figure 2 depicts phase diagrams with progressively higher resolution for the dynamical system defined by the equations

$$\dot{x} = -y - z, \quad (1)$$

$$\dot{y} = x + ay, \quad (2)$$

$$\dot{z} = bx + z(x - c), \quad (3)$$

where a , b , c are control parameters. This is one of the prototypical models introduced by Rössler [1976, 1979a, 1979b] to mimic continuous-time chaos. In the literature, all these models are referred to indistinctly as “Rössler’s oscillators”. The above normal form was investigated previously by Fraser and Kapral [1982], who reported a phase diagram displaying a few stability boundaries for oscillations with the simplest waveforms.

We computed the Lyapunov spectra for Eqs. (1)–(3) after fixing $b = 0.4$ and integrating them for a rectangular mesh of typically 800×800 points in parameter space, using a fourth-order Runge–Kutta scheme with fixed integration step, mostly $h = 0.01$. The first 35×10^3 steps were discarded, the subsequent 700×10^3 steps were used to compute the Lyapunov spectra. We used our in-house FORTRAN software to plot 8-bit compressed color PostScript bitmaps directly

from the Lyapunov spectra [Gallas, 1993, 1995]. As usual, the largest nonzero exponents were then used to discriminate periodicity from chaos, producing PostScript phase diagrams like those in Fig. 2.

Chaotic oscillations (i.e. positive exponents) are represented using colors while periodic oscillations (negative exponents) are shown using a gray scale, as indicated by the color scale. The color scale is linear on both sides of zero but is not uniform from minimum to maximum exponent. In other words, the scales of colors and of gray shadings are linear on both sides of zero but are independent from each other. Furthermore, the scales of each individual phase diagram were always renormalized to reflect the corresponding minima and maxima of the diagram. That is why colors of identical structures may look slightly different from panel to panel, when enlarged. The pink shading denotes parameters producing mostly divergent solutions. Figure 2 shows

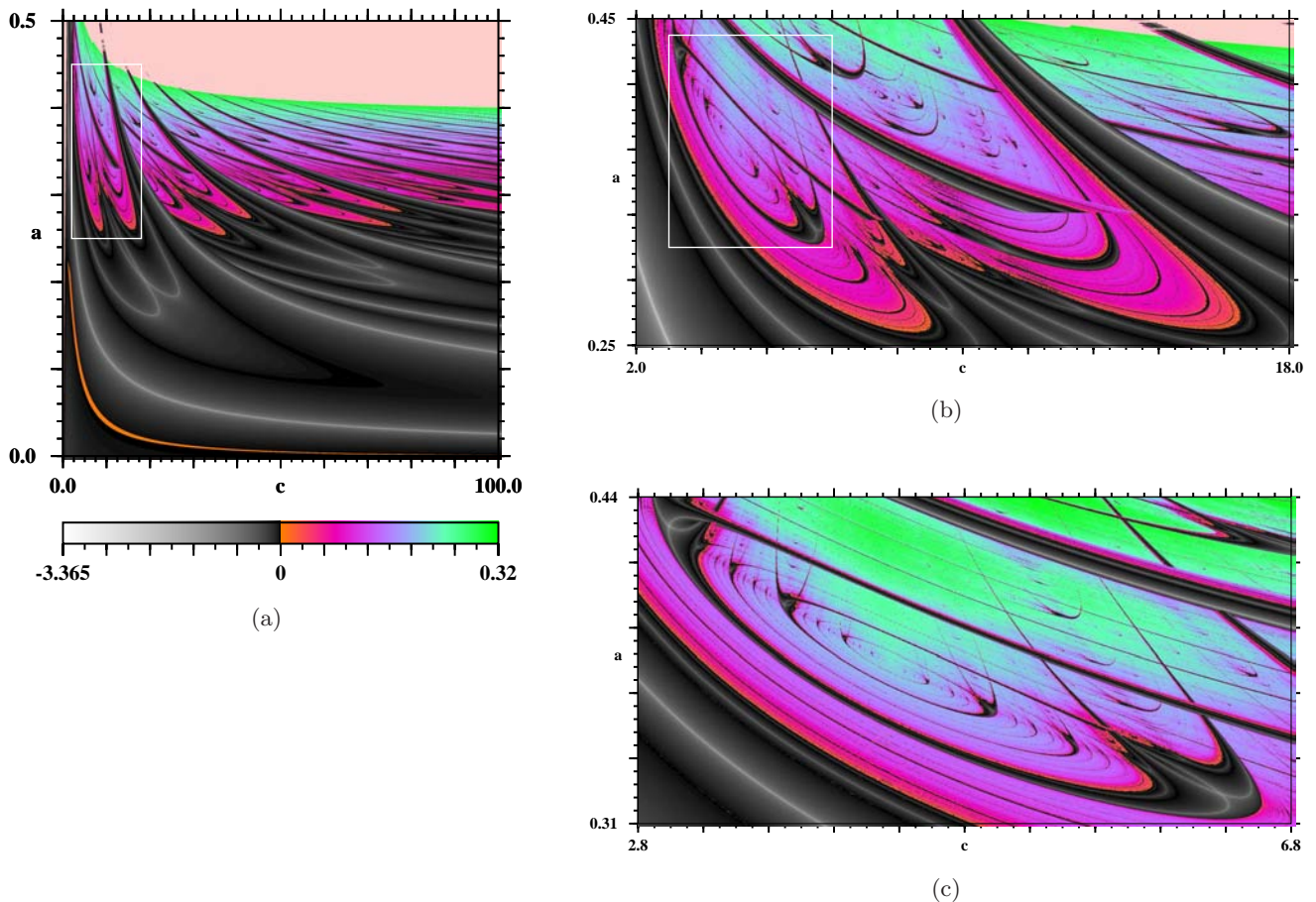


Fig. 2. Progressively more highly resolved phase diagrams displaying a hub, more easily seen in (c), for Rössler’s equations in Eqs. (1)–(3), with $b = 0.4$. The pink shading denotes parameters producing mostly divergent solutions. The colors of individual panels vary because the color scale is not fixed, but is renormalized to reflect minima and maxima of individual panels. Note the repetition in the leftmost panel of the “double-well” looking structure seen in (b). The boxes are shown magnified in the next panels. This figure is motivated by Fig. 1 of [Fraser & Kapral, 1982]. Resolution: 2000×2000 exponents.

our first example of an isolated hub in a dynamical system with continuously differentiable equations of motion. The hub and its infinite spirals is more clearly seen in Fig. 2(c). The organization is the same as found in piecewise-linear circuits [Bonatto & Gallas 2008; Ramírez-Ávila & Gallas 2008, 2009]. This fact shows that hubs are not artifacts arising from discontinuities in derivatives.

Figure 3 depicts analogous phase diagrams for a second normal form of a Rössler oscillator, namely,

$$\dot{x} = -y - z, \tag{4}$$

$$\dot{y} = x + ay, \tag{5}$$

$$\dot{z} = b + z(x - c), \tag{6}$$

where a, b, c are parameters. The only difference between both models is the term involving b in the \dot{z} equation. We will focus on the latter model because Eq. (6) contains one multiplication less than Eq. (3) and, therefore, is faster to evaluate repeatedly during extended computations. Both normal forms produce equivalent results in the sense that they display analogous hubs, as may be seen by

comparing Figs. 2 and 3. Each panel in Fig. 3 displays phase diagrams computed as before, for grids of 800×800 equally spaced parameter points.

From Fig. 3, one recognizes two distinctive signatures: (i) an infinite *nesting of spirals* corresponding to periodic solutions, and (ii) the presence of a remarkable *focal point* where all spirals originate/terminate and which seems to “organize” the dynamics in a wide portion of the parameter space around it. Individual spirals originating/terminating at the focal hub are characterized by specific *families of periodic oscillations* embedded in the chaotic phase. Spirals and the spiral nesting are truly codimension-two phenomena: they may be only fully unfolded by tuning two or more parameters simultaneously. *Mutatis mutandis*, there are also white spirals of chaos.

Figure 3 reveals a number of different features when compared with the organization seen around the hubs of piecewise electrical circuits [Bonatto & Gallas, 2008; Ramírez-Ávila & Gallas, 2008, 2009]. The most salient one is the left–right asymmetry seen under the large four legged “shrimp-like”

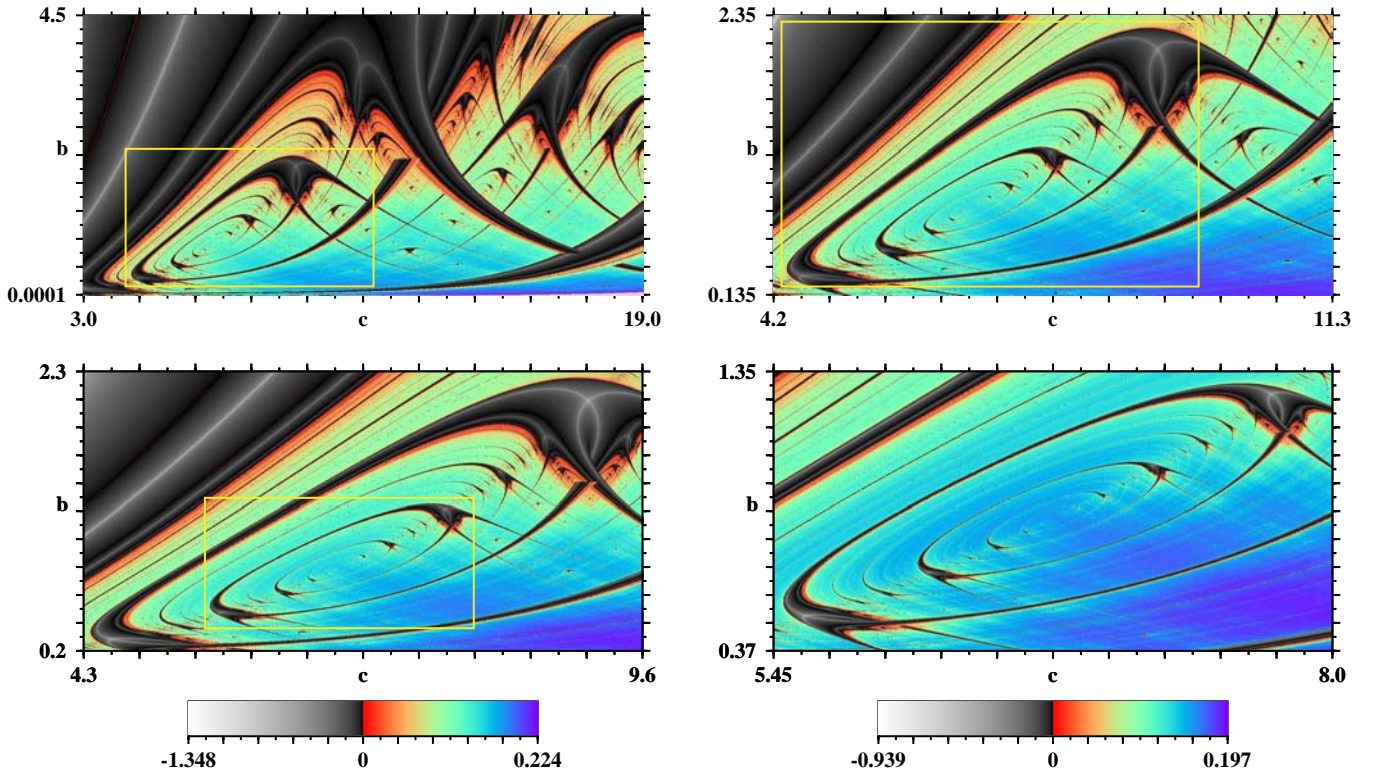


Fig. 3. Phase diagrams for Rössler equations, Eqs. (4)–(6) with $a = 0.25$, showing the location of a focal hub and the infinite sequence of spirals connected to it. The focal hub is located roughly at the center of infinite sequence of spirals seen in the lower-right panel. Boxes denote parameter regions being magnified successively. Colors indicate domains of positive exponents while absence of colors denotes periodicity (negative Lyapunov exponents). The colors of each individual panel was renormalized to display the minimum and maximum exponents contained in them, as indicated by the color scales.

structure [Gallas 1993, 1994, 1995; Lorenz 2008] located inside the top-right box in Fig. 3(a): while the left side of the shrimp-like structure contains a hub and the corresponding nesting of spirals, the right side contains no hub at all. Additionally, in Fig. 3(c) it is possible to recognize that the focal hub is located roughly at the intersection of the pair of diagonals of the rectangular white box. The main diagonal is located roughly parallel to an axis of approximate reflection symmetry which becomes more and more accurate as one approaches more and more the focal hub. In contrast, a line parallel to the secondary diagonal and passing through the hub divides the parameter plane into (i) an upper region of quite tame behaviors, where bifurcation diagrams along any line passing through the hub display the same structure, and (ii) a region of more complicated dynamics, below the diagonal, which may be subdivided into two regions which approximately “mirror” each other along the approximate axis of symmetry. The dynamical structuring and some metric properties of the three regions around the hub of Rössler’s equations will be discussed elsewhere. A natural question here is: Why spiralling “takes sides”? That is, what is the reason for a preferential spiralling to happen in specific regions of the parameter spaces, apparently avoiding to emerge in a more symmetrically arranged form covering both sides?

Figure 4 illustrates the hub evolution when the remaining control parameter a is tuned in Eqs. (4)–(6). It shows sections of the intricate hub surface in parameter space, in particular, its two limiting orientations found for small and large values of a . Such limit situations are interesting because they allow a number of exact analytical results to be obtained. Figure 4 corroborates a natural expectation: that all curves in Fig. 1 are in fact just low-dimensional sections of *extended surfaces* living in the higher multidimensional parameter space.

At least numerically, the regular structuring around hubs as well as their accumulation properties seem to be invariant for all hubs discovered so far. A distinctive feature observed sometimes is a pronounced “bending asymmetry”: the shrimp distortion is far greater in one side of the symmetry line S than on the other side. Figure 5 illustrates this bending asymmetry. Bending asymmetries might be due to “nonoptimal” positioning of the hub structure in the multidimensional parameter space. Since no theoretical help exists to locate hubs, it is helpful to have a good idea of the possible spatial orientation and extension of hub to more easily locate them in arbitrary multidimensional spaces. A detailed investigation of this positioning is quite time-consuming but is certainly necessary to elucidate what to expect for sections of the parameter space.

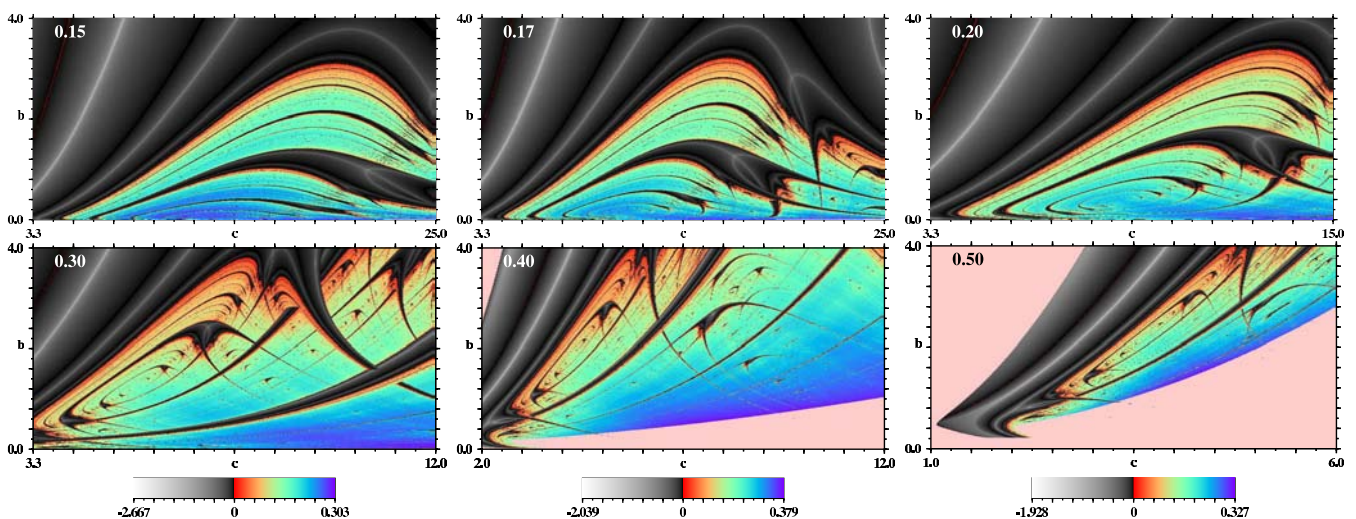


Fig. 4. Evolution of the hub and spirals in the $c \times b$ phase diagram as a function of a , indicated inside each panel, for Rössler’s oscillator of Eqs. (4)–(6). Colors denote chaos (positive Lyapunov exponents) while dark shadings denote periodicity (negative exponents). The pink regions seen for $a = 0.40$ and 0.50 indicate predominance of divergence. The color scales of individual panels were renormalized to reflect the minimum and maximum exponents of each panel, as illustrated by the scales in the bottom row. Note differences in horizontal axis, indicating a significant compression when a grows.

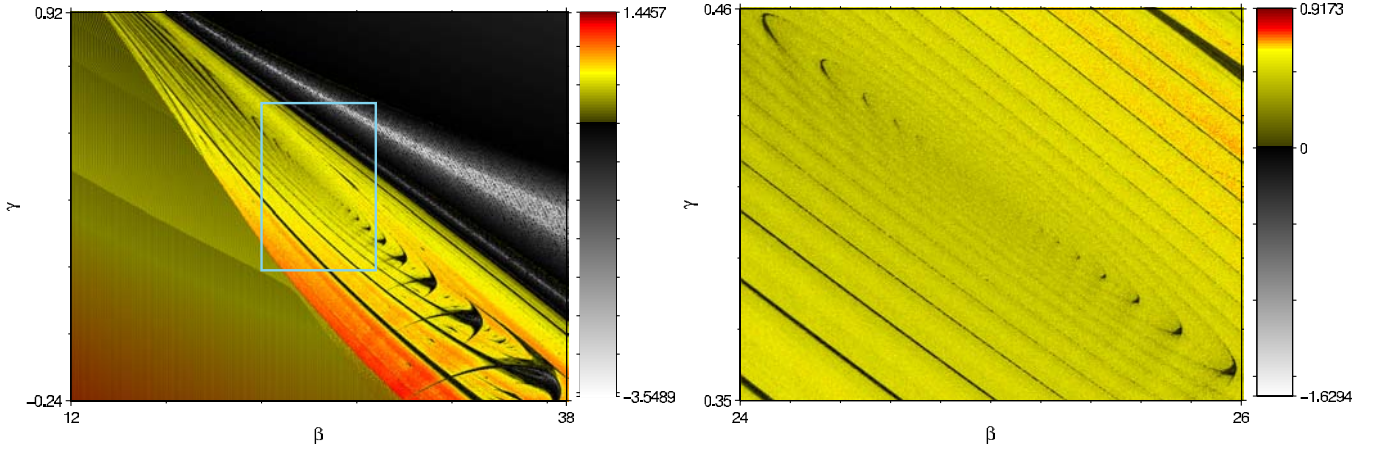


Fig. 5. Hub for Chua’s circuit with piecewise linear term. Note the strong bending asymmetry of the shrimp shapes on distinct sides of the hub. Similar asymmetries exist when the piecewise linear term is replaced by a cubic nonlinearity in the circuit. For details about this figure and hubs for Chua’s circuit see [Ramírez-Ávila & Gallas, 2008, 2009].

Before proceeding, we mention briefly two very important works by Gaspard and collaborators [1983, 1984] where the parameter space of Eqs. (1)–(3) was analyzed. They focus on *unstable* homoclinic orbits related with a theorem of L. Shilnikov, not on experimentally accessible *stable* orbits as done here. Moreover, we mention that while it is tempting to associate spiral nestings with the much studied homoclinic orbits, we have found spirals not to be numerically detectable in some flows which are textbook examples of the Shilnikov setup. This will be discussed elsewhere. As mentioned in the introduction, periodicity hubs emerge at certain bendings, or foldings, of homoclinic loci in parameter space. Their *local* structure is essentially as nicely described more than a quarter century ago by Gaspard *et al.* [1983, 1984]. Their *global* organization is considerably more complex and a first account was provided recently by Vitolo *et al.* [2009]. To conclude this section, we mention that it is possible to identify periodicity hubs in some figures contained in papers published recently, e.g. [Castro *et al.*, 2007; Albuquerque *et al.*, 2008]. Such works, however, contain no reference to hubs and their roles.

3. Infinite Hub Cascades in a Chemical Oscillator

The purpose of this section is to show that hubs may also arise in infinite cascades with subcascades, *ad infinitum*. Such ordered cascading and subcascading may be recognized in the sequences of magnifications depicted in Figs. 6 and 7. The hierarchical cascading seems to be connected to a *master hub* which acts like a sort of source for

an infinite hub network. The accumulation process underlying hub cascades leads to characteristic parameter paths, loci, with remarkably fertile structure. Every individual hub is the termination of a family of periodic orbits as their period grows more and more, diverging without any bound, and their waveform evolves continuously.

Figures 6 and 7 illustrate specific sections of the control parameter space for a polynomial chemical model studied by Gaspard and Nicolis [1983]. In this model, the temporal evolution of certain chemical concentrations (x, y, z) is governed by three coupled nonlinear differential equations derived from the mass action law of chemical kinetics:

$$\dot{x} = (\beta x - f y - z + g)x, \quad (7)$$

$$\dot{y} = (x + s z - \alpha)y, \quad (8)$$

$$\varepsilon \dot{z} = x - a z^3 + b z^2 - c z. \quad (9)$$

Following Gaspard and Nicolis, we investigate the $\alpha \times \beta$ parameter plane while keeping all other parameters fixed at the following values: $a = 0.5$, $b = 3$, $\varepsilon = 0.01$, $f = 0.5$, $g = 0.6$, $s = 0.3$, but taking $c = 4.8$ for better visibility of the hubs.

Figure 6 shows a large portion of the $\alpha \times \beta$ plane where, in panels (a) and (b), it is easy to recognize infinite sequences of hubs and spirals “irradiated” from a master hub located roughly at the center of the rectangle at the bottom of Fig. 6(b), with approximate coordinates

$$(\alpha_m, \beta_m) = (0.7825, 0.39213). \quad (10)$$

This point may be identified at the bottom of Fig. 6(f) and at the center of Fig. 7. Its location may

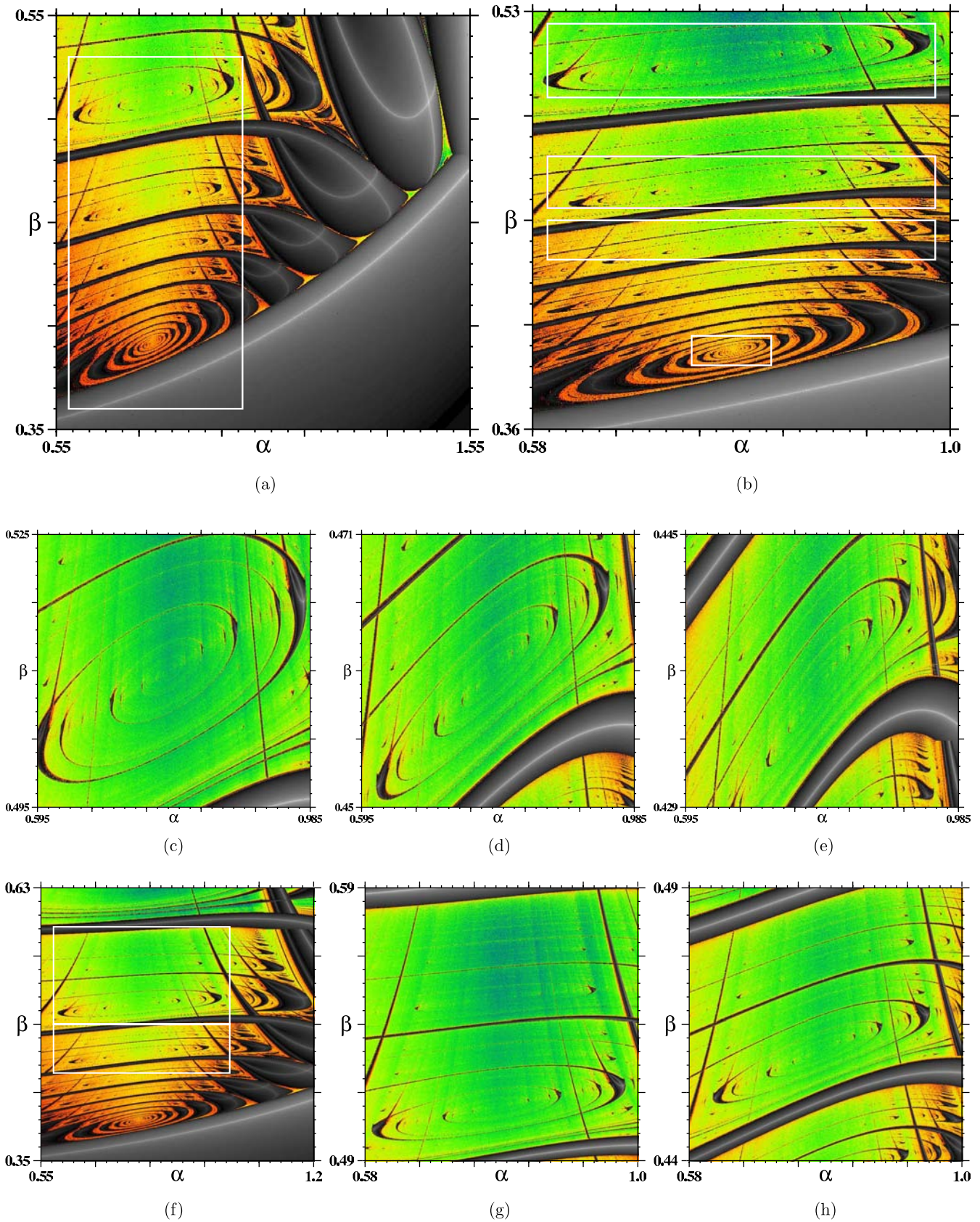


Fig. 6. Lyapunov phase diagram for the chemical model of Eqs. (7)–(8) displaying infinite hierarchies of focal hubs, each surrounded by its corresponding spiral nestings. Top row: global views. The smaller box in panel (b) is shown magnified in Fig. 7. Middle row: Zoom of the three larger boxes seen in (b). Bottom row: Infinite sequences of hubs. (g) and (h) show the infinite hub networks contained in the pair of boxes in (f).

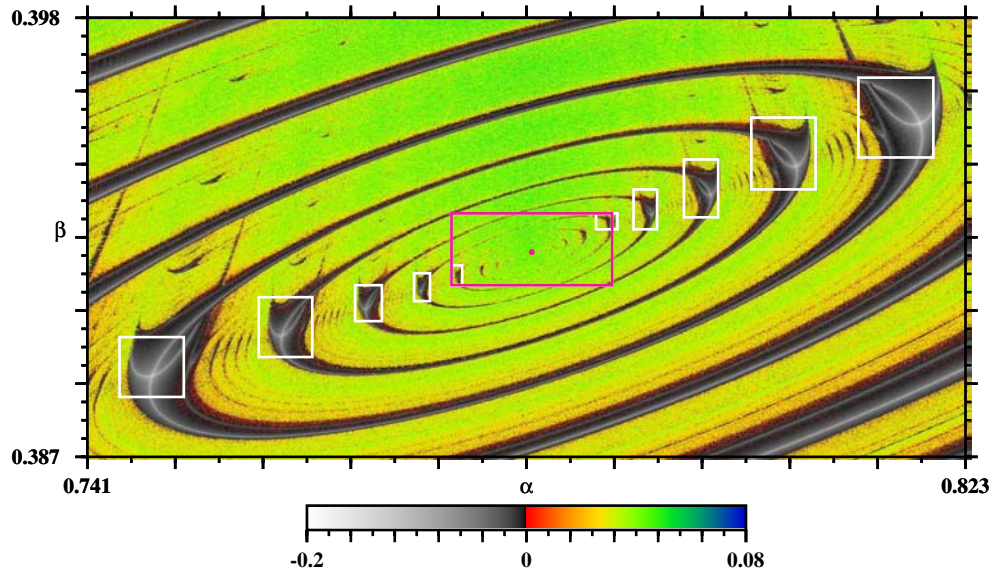


Fig. 7. Phase diagram illustrating the convergence towards the “master hub”, located roughly at the red dot with coordinates given in Eq. (10), near the center of the central pink box. The intersections of “superstable” loci inside the white boxes may be used to estimate the position of the master hub.

be estimated by considering the intersection of consecutive pairs of straight lines, one on the left and other on the right of the central hub. Such pairs of lines pass through the *superstable* intersection of the parabolae located inside the white boxes in Fig. 7 and which quickly become hard to distinguish in the figure. The precise coordinates of (α_m, β_m) are obtained in the infinite limit when the straight lines converge towards the focal hub, degenerating there to a point. Equation (10) provides just an estimate of the final accumulation point.

An interesting feature that should deserve further consideration is the relative similarity of the three phase diagrams shown in Figs. 6(c)–6(e).

Although no effort was made to find adequate viewing windows for these figures, their close resemblance seems to indicate that simple *affine transformations* similar to the ones used to superimposed domains of stable periodicities in one-dimensional two-parameter discrete-time dynamical systems [Gallas, 1994; Hunt *et al.*, 1999] should allow one to find “parametrically isomorphic domains” much in the same spirit of those recently reported by Bonatto *et al.* [2008].

Gaspard and Nicolis [1983] reported in their Fig. 9 a phase diagram for Eqs. (7)–(8). Their diagram consists of three line segments: one identified as the homoclinic locus of one of the fixed points

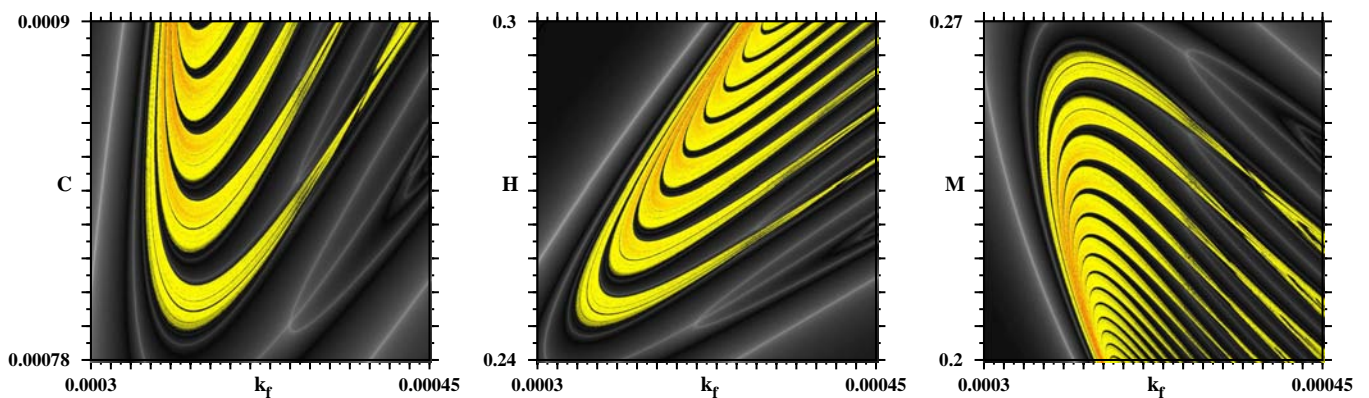


Fig. 8. Sequences of phase diagrams displaying “fountains” of chaos in three distinct sections of the 14-dimensional parameter space of the nonpolynomial model originally found by Györgyi and Field [1992] to reproduce chaos in the Belousov–Zhabotinsky reaction. Such structures resemble half-cuts of the structure containing a hub. For details see [Freire *et al.*, 2009].

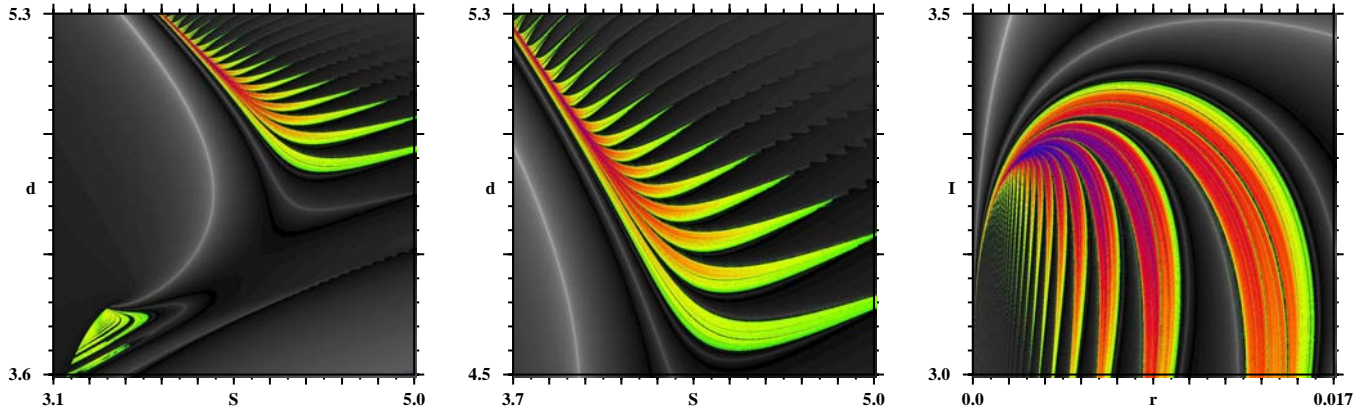


Fig. 9. Sequences of phase diagrams displaying “fountains” of chaos for the Hindmarsh–Rose [1984] neuronal model, Eqs. (11)–(13), with $a = 1$, $b = 3$, $c = 1$, $d = 5$, $S = 4$, $r = 0.003$, $I = 3.31$, and $x_1 = -1.6$. Such structures resemble half-cuts of the structure containing a hub. Similar fountains were also found in other models. For details see [Freire & Gallas, 2009].

of the system, one identified as the line where a certain limit cycle loses its stability and a Hopf bifurcation line. Their homoclinic locus seems to lie close in our Fig. 6 to what was defined as the characteristic direction h (defined in Fig. 1), along which all major shrimp legs not coiling up around the main hub sequence accumulate. A one-dimensional map model of the situation is discussed by Gaspard *et al.* [1984].

As shown by Figs. 6(a) and 6(b), the relevant dynamical fact here is that the roughly vertical line containing infinite hubs *results* from the severe constraint imposed by accumulation processes involving two families of *stable* shrimp legs, one on the left, one on the right of the vertical hub line. In Figs. 6(a) and 6(b) the vertical line corresponds to the accumulation line h defined in Fig. 1. In other words, such line seems not to be a *source* of interesting dynamics but, instead, to simply arise from the leg accumulation process. Gaspard and Nicolis also briefly mention a certain point M , terminal point of a homoclinic locus, without much discussion. As illustrated by Fig. 7, the master hub acts as a sort of sun having infinite layers of shrimps, its “planets”, orbiting in spirals around it. Each spiral, either of periodicity or of chaos, is characterized by specific oscillatory pattern. The master hub behaves like a busy commuting center where, after following a spiral characterized by a specific pattern, one may commute to any other of the infinite patterns available there. It is possible to jump from an oscillatory to a chaotic pattern or vice-versa. Noise may allow the commutation to occur much earlier than reaching the master hub. While unstable homoclinic loci are certainly interesting mathematical players

closely linked to the complex dynamics, we focus on a description based on stable oscillatory patterns that can be directly measured in experiments.

To conclude this section, we present in Figs. 8 and 9 very interesting structures, “fountains of chaos”, resembling half-cuts of the arrangement around hubs. They are shown here for two rather distinct models, namely a 14-parameter nonpolynomial model of the Belousov–Zhabotinsky reaction proposed by Györgyi and Field [1992] and the eight-parameter Hindmarsh–Rose [1984] model of neuronal spiking and bursting:

$$\frac{dx}{dt} = y - ax^3 + bx^2 + I - z, \quad (11)$$

$$\frac{dy}{dt} = c - dx^2 - y, \quad (12)$$

$$\frac{dz}{dt} = [(x - x_1)S - z]r. \quad (13)$$

This type of structure may be indicative of a nearby hub and motivate the exploration of high-dimensional parameter spaces.

4. T -Point Spirals versus Hub Spirals

The aim of this section is to answer the following question: are hub spirals connected in some way to the spirals known to exist near T -points? We have not yet been able to find any connection between them. Our most direct attempt to correlate both sets of spirals is described in the remainder of this section.

There are studies in the literature about certain heteroclinic bifurcations in the paradigmatic Lorenz

equations which have also described families of spirals winding up around *terminal points*, or *T*-points, in parameter space. Such points are defined by degeneracies between stable and unstable manifolds of distinct fixed points [Alfsen & Frøyland, 1985; Glendinning & Sparrow, 1986; Bykov, 1993; Shilnikov, 1993]. Thus, it is natural to look for connections between the spirals from these earlier studies and the infinite sequences of spirals connected with periodicity hubs.

The earlier studies involve essentially the use of standard techniques to derive return maps near fixed points. Such techniques provide first-order results valid locally, near “sufficiently small” neighborhoods of stationary points where the flow may be assumed as linear to be solved analytically. As pointed out by Glendinning and Sparrow [1986], there are a number of restrictions for their validity, even when confined just to the Lorenz equations.

A *T*-point was studied numerically in detail by Shilnikov [1997] for the following model:

$$\dot{x} = y, \quad (14)$$

$$\dot{y} = x(1 - z) - Bx^3 - by, \quad (15)$$

$$\dot{z} = -a(z - x^2), \quad (16)$$

where we use a instead of the original α and b instead of λ , to avoid confusion with the symbols used earlier for Lyapunov exponents. As pointed out by Shilnikov, the model above displays various scenarios involving appearance and destruction of chaos and bifurcations of chaotic regimes typical for some three-level laser models. For this reason, we refer to this model as Shilnikov’s laser model.

For $B = 0$, A. Shilnikov computed the phase diagram shown in the left panel of Fig. 10, where the location of a *T*-point and two spirals is indicated. The corresponding Lyapunov phase diagram computed as described in Sec. 2 is shown in the right panel. Comparison of both figures shows their content to be quite different. In particular, the Lyapunov diagram shows no sign of the spirals accumulating on the *T*-point of the left panel. To investigate this question further, Fig. 11 presents several magnifications of the chaotic phase of Shilnikov’s model. Figures 10 and 11 seem to provide evidence that the spirals accumulating in *T*-points and the spirals accumulating in hubs are of a quite distinct nature because they produce very different phase diagrams. Curiously, both situations deal with infinite spiral structures and sequences of codimension

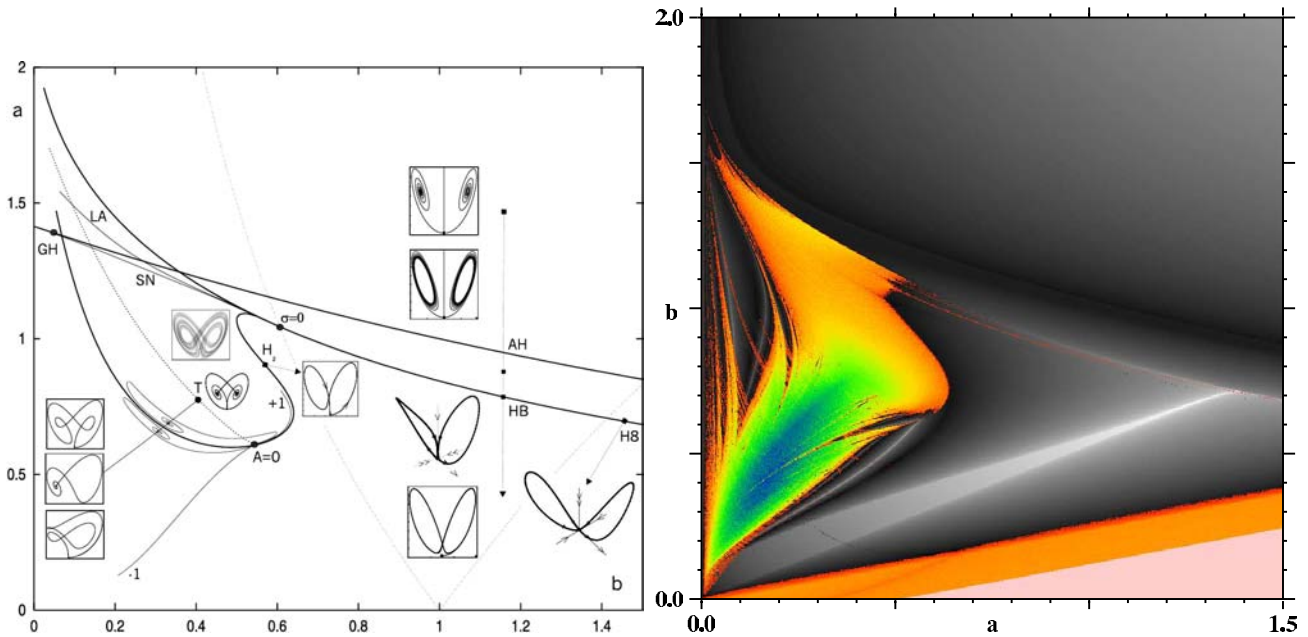


Fig. 10. Left panel: Phase diagram for the Shimizu–Morioka laser model, Eq. (15) with $B = 0$, reproduced with permission from [Shilnikov *et al.*, 2001], where its details are explained. *T* marks the location of the *T*-point discussed in the text. Right panel: Lyapunov phase diagram displaying 800×800 exponents. Colors indicate domains of chaos (i.e. positive Lyapunov exponents) while absence of colors marks periodicity (negative exponents). The pink triangle in the lower right corner denotes divergent solutions. The overall cartographic description provided by these figures is rather distinct, both in emphasis and details. The panel on the right characterizes domains of *stable* orbits, with basins of attraction having positive measure. The large homogeneous chaotic phase seen in the rightmost panel is shown with greater detail in Fig. 11.

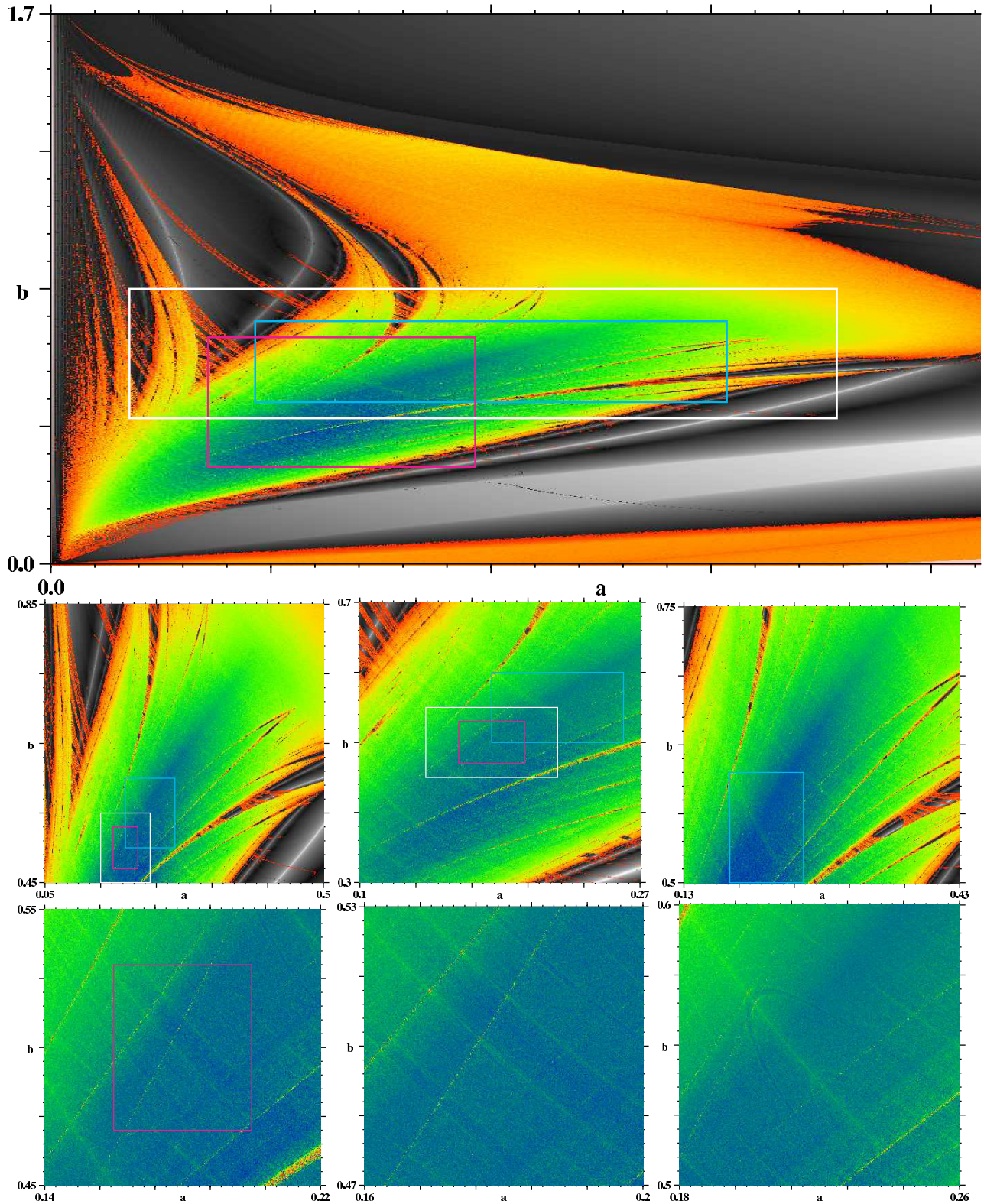


Fig. 11. Sequences of phase diagrams for the Shimizu–Morioka model of a homogeneously broadened single-mode laser, Eq. (15) with $B = 0$. Macroscopically, the model displays a surprisingly large *homogeneous chaotic phase*, but no trace of a hub and spirals in the region where it is known to contain a T -point (shown in Fig. 10; see text). The colors in each individual panel were renormalized to reflect the minimum and maximum exponents contained in them. In the middle row: The white box highlights the region $a \in [0.14, 0.22] \times b \in [0.45, 0.55]$. The magenta box highlights the region $a \in [0.16, 0.20] \times b \in [0.47, 0.53]$. The cyan box highlights the region $a \in [0.18, 0.26] \times b \in [0.50, 0.60]$. The panels in the bottom row show magnifications of these three boxes. The top panel displays 800×800 exponents while each of the six smaller panels shows 400×400 exponents.

two points approaching certain “fundamental” codimension two points. This subject certainly deserves further study and the development of an adequate theoretical foundation.

For physical applications, a key point is that the Lyapunov phase diagram reflects macroscopically *stable* dynamical phenomena, characterized by positive-measure basins of attraction in phase space. In contrast, the fundamental loci due to the *unstable* oscillations underlying *T*-points are not easily measurable. Unstable orbits have basins of attraction with measure-zero, being considerably more difficult to locate. All hubs are termination points of infinite families of stable periodic orbits of ever evolving waveforms and periods growing continuously without any upper bound, diverging to infinity.

5. Laser Chaos: Dense, Homogeneous or Robust?

The recent demonstration of the feasibility of a purely hardware level encryption scheme based on chaos in communications over 120 km of a commercial fiber-optic channel in the metropolitan area network of Athens, Greece [Argyris *et al.*, 2005] has attracted renewed attention to great potential of path-breaking applications of chaotic laser signals. Of importance for such applications is to find wide parameter regions characterized by *dense chaos* and a total absence of periodic windows embedded in them.

The notion of “robust chaos” has been used in the literature to describe dense, or equivalently, homogeneous chaos, i.e. chaos with no periodic windows embedded in it, like that found for the Shilnikov model of Eqs. (14)–(16) and represented in Figs. 10 and 11. Robust chaos was discussed in 1992–94 by Majumdar and Mitra [1994] while studying dynamic optimization models. These authors expressed the opinion that chaos occurs for non-negligible set of parameter values and, therefore, cannot be dismissed as “accidental” for families of economies. Subsequently, the notion of robust chaos was introduced again by Banerjee *et al.* [1998], motivated by practical applications demanding chaotic orbits characterized by the absence of periodic windows and coexisting attractors in some neighborhood of parameter space. A plethora of systems are well-known for the absence of periodic regions in chaotic phases, mostly discrete maps [Kawabe & Kondo, 1991a, 1991b, 1993; Cosenza &

Gonzalez 1998; Potapov & Ali, 2000; Priel & Kanter, 2000; Andreut & Ali, 2001; Alvarez-Llamoza *et al.*, 2008]. An overview of some issue related with dense chaos for maps was presented recently by Elhadj and Sprott [2008].

Although the name robust chaos has been in use, we feel perhaps belatedly that it is not adequate. In mathematics, the topological notions attached to the words *dense* or *connected* seem more appropriate to describe the absence of periodic windows embedded in chaos. In physics, the notion of robustness is traditionally attached to perturbation theory, to stability in phase-space, not to phase diagrams. Robust means resistant to perturbations. In physics, phase diagrams have *homogeneous phases* which are necessarily robust. Otherwise, they could not be directly observed experimentally. For this reason, we prefer to say *dense chaos* or, equivalently, *homogeneous chaos*, the traditional names of statistical physics adapted to the situation.

The chaotic phase seen in Figs. 10 and 11 for the Shilnikov model is the largest homogeneous chaotic phase that we are aware of for a flow. From a practical point of view, it is clear that dense chaos like that in Fig. 11 is potentially interesting for a number of applications, for instance, for real-time digital secure communications with encrypted signals using the chaotic output of semiconductor lasers as carriers.

6. Conclusions

We have studied the evolution of infinite families of periodic oscillations embedded in chaotic phases of simple flows, i.e. dynamical systems ruled by systems of ordinary differential equations. The chaotic phases of prototypical dynamical systems were shown to contain a characteristic hub towards which an infinite sequence of spirals representing periodic oscillations converge. We presented a simple chemical flow that contains an infinite of cascades and subcascades of hubs and spirals, all organized in a quite regular way, as shown in Fig. 6. All hubs are termination points of an infinite family of periodic orbits of ever evolving waveforms as its period becomes infinite. Infinite hub cascades were also found in the piecewise-linear circuits of Sec. 1 and in other systems. In fact, it may well be that infinite hub cascade are always present, being just simpler to recognize in some flows than in others.

On the basis of evidence provided by a model introduced by Shilnikov, we have argued that hubs

are codimension-two points of a different nature than the so-called T -points. Hubs involve global bifurcations of *stable* orbits and seem to require more elaborate analytical ingredients for their theoretical description than the usual linear stability analysis around fixed points. It is our hope that the surprisingly rich examples described here will stimulate analytical developments.

Complex systems are sometimes characterized by the concept of “emergence”, associated with systems displaying organization without a central organizing authority [Ottino, 2004]. In this sense, systems containing hubs should not to be regarded as complex. However, as shown for several distinct dynamical systems here, the presence of powerful networks of stable “organizing authorities” of positive measure may remain undetected for long time, despite decades of intensive work.

Acknowledgments

The author thanks Hans J. Herrmann for a very fruitful month spent in Zürich. He also thanks Paul Glendinning and Andrey Shilnikov for pointing out independently that T -points might be connected with hubs, for helpful email exchanges, and A. Shilnikov for his kind permission to reproduce the phase diagram of Shilnikov *et al.* [2001]. This work was supported by the Air Force Office of Scientific Research, Contract FA9550-07-1-0102, and by CNPq, Brazil. Most of the computations were done on the SUN Fire X2200 and X4600 clusters of the CESUP-UFRGS.

References

- Albuquerque, H. A., Rubinger, R. M. & Rech, P.C. [2008] “Self-similar structures in a 2D parameter-space of an inductorless Chua’s circuit,” *Phys. Lett. A* **372**, 4793–4798.
- Alfsen, K. H. & Frøyland, J. [1985] “Systematics of the Lorenz model at $\sigma = 10$,” *Phys. Scripta* **31**, 15–20.
- Alvarez-Llamoza, O., Cosenza, M. G. & Ponce, G. A. [2008] “Critical behavior of the Lyapunov exponent in type-III intermittency,” *Chaos Solit. Fract.* **36**, 150–156.
- Andrecut, M. & Ali, M. K. [2001] “Robust chaos in smooth unimodal maps,” *Phys. Rev. E* **64**, 025203R.
- Argyris, A., Syvridis, D., Larger, L., Annovazzi-Lodi, V., Colet, P., Fischer, I., García-Ojalvo, J., Mirasso, C. R., Pesquera, L. & Shore, K. A. [2005] “Chaos-based communications at high bit rates using commercial fiber optics,” *Nature* **438**, 343–346.
- Banerjee, S., Yorke, J. A., & Grebogi, C. [1998] “Robust chaos,” *Phys. Rev. Lett.* **80**, 3049–3052.
- Bonato, C. & Gallas, J. A. C. [2007] “Accumulation horizons and period adding cascades in optically injected semiconductor lasers,” *Phys. Rev. E* **75**, 055204(R).
- Bonato, C. & Gallas, J. A. C. [2008a] “Periodicity hub and nested spirals in the phase diagram of a simple resistive circuit,” *Phys. Rev. Lett.* **101**, 054101.
- Bonato, C. & Gallas, J. A. C. [2008b] “Accumulation boundaries: Codimension-two accumulation of accumulations in phase diagrams of semiconductor lasers, electric circuits, atmospheric, and chemical oscillators,” *Phil. Trans. Royal Soc. London, Series A* **366**, 505–517.
- Bonato, C., Garreau, J. C. & Gallas, J. A. C. [2005] “Self-similarities in the frequency-amplitude space of a loss-modulated CO₂ laser,” *Phys. Rev. Lett.* **95**, 143905.
- Bonato, C., Gallas, J. A. C. & Ueda, Y. [2008] “Chaotic phase similarities and recurrences in a damped-driven Duffing oscillator,” *Phys. Rev. E* **77**, 026217.
- Bykov, V. V. [1993] “The bifurcation of separatrix contours and chaos,” *Physica D* **62**, 290–299.
- Castro, V., Monti, M., Pardo, W. B., Walkenstein, J. A., & Rosa, Jr. E [2007] “Characterization of the Rössler system in parameter space,” *Int. J. Bifurcation and Chaos* **17**, 956–973
- Cosenza, M. G. & González, J. [1998] “Synchronization and collective behavior in globally coupled logarithmic maps,” *Prog. Theor. Phys.* **100**, 21–38.
- Elhadj, Z. & Sprott, J. C. [2008] “On the robustness of chaos in dynamical systems: Theories and applications,” *Front. Phys. China* **3**, 195–204.
- Franceschetti, D. R. [1999] *Biographical Encyclopedia of Mathematicians* (Marshall Cavendish, Tarrytown NY).
- Fraser, S. & Kapral, R. [1982] “Analysis of flow hysteresis by a one-dimensional map,” *Phys. Rev. A* **25**, 3223–3233.
- Freire, J. G., Bonatto, C., DaCamara, C. & Gallas, J. A. C. [2008] “Multistability, phase diagrams, and intransitivity in the Lorenz-84 low-order atmospheric circulation model,” *Chaos* **18**, 033121.
- Freire, J. G. & Gallas, J. A. C [2009] “Distribution of periodic and chaotic bursting in Hindmarsh–Rose neuronal activity,” in preparation.
- Freire, J. G., Gallas, J. A. C & Field, R. J. [2009] “Relative abundance and structure of chaotic behavior: The nonpolynomial Belousov–Zhabotinsky reaction kinetics,” *J. Chem. Phys.* **131**, 044105.
- Gallas, J. A. C. [1993] “Structure of the parameter space of the Hénon map,” *Phys. Rev. Lett.* **70**, 2714–2717.
- Gallas, J. A. C. [1994] “Dissecting shrimps: results for some one-dimensional physical systems,” *Physica A* **202**, 196–223.

- Gallas, J. A. C. [1995] “Structure of the parameter space of a ring cavity,” *Appl. Phys. B* **60**, S203–S213. Special issue dedicated to the 60th birthday of Herbert Walther; see also Zeni, A. R. & Gallas, J. A. C. [1995] “Lyapunov exponents for a Duffing oscillator,” *Physica D* **89**, 71–82.
- Gaspard, P. & Nicolis, G. [1983] “What can we learn from homoclinic orbits in chaotic dynamics?” *J. Stat. Phys.* **31**, 499–518.
- Gaspard, P., Kapral, R. & Nicolis, G. [1984] “Bifurcation phenomena near homoclinic systems: A two-parameter analysis,” *J. Stat. Phys.* **35**, 697–727.
- Glendinning, P. & Sparrow, C. [1986] “*T*-points: A codimension two heteroclinic bifurcation,” *J. Stat. Phys.* **43**, 479–488.
- Gonchenko, S. V., Ovsyannikov, I. I., Simó, C. & Turaev, D. [2005] “Three-dimensional Hénon-like maps and wild Lorenz-like attractors,” *Int. J. Bifurcation and Chaos* **15**, 3493–3508.
- Györgyi, L. & Field, R. J. [1992] “A three-variable model of deterministic chaos in the Belousov–Zhabotinsky reaction,” *Nature* **355**, 808–810.
- Hindmarsh, J. L. & Rose, R. M. [1984] “A model of neuronal bursting using three coupled first order differential equations,” *Proc. Royal Soc. London B* **221**, 87–102.
- Hunt, B. R., Gallas, J. A. C., Grebogi, C., Yorke, J. A. & Koçak, H. [1999] “Bifurcation rigidity,” *Physica D* **129**, 35–56.
- Ince, E. L. [1926] *Ordinary Differential Equations*, (Longmans, Green and Co., London), reprinted since 1956 by Dover, Mineola,
- Kawabe, T. & Kondo, Y. [1991a] “Fractal transformation of the 1d chaos produced by logarithmic map,” *Prog. Theor. Phys.* **85**, 759–769.
- Kawabe, T. & Kondo, Y. [1991b] “Intermittent chaos generated by logarithmic map,” *Prog. Theor. Phys.* **86**, 581–586.
- Kawabe, T. & Kondo, Y. [1993] “Bifurcations of the complex logarithmic map,” *J. Phys. Soc. Japan* **62**, 497–505.
- Lorenz, E. N. [2008] “Compound windows of the Hénon map,” *Physica D* **237**, 1689–1704.
- Majumdar, M. & Mitra, T. [1994] “Robust chaos in dynamic optimization models,” *Ricerche Economiche* **48**, 225–240.
- Martins, L. C. & Gallas, J. A. C. [2008] “Multistability, phase diagrams and statistical properties of the kicked rotor: a map with many coexisting attractors,” *Int. J. Bifurcation and Chaos* **18**, 1705–1717.
- Ottino, J. M. [2004] “Engineering complex systems,” *Nature* **427**, 399.
- Potapov, A. & Ali, M. K. [2000] “Robust chaos in neural networks,” *Phys. Lett. A* **277**, 310–322.
- Priel, A. & Kanter, I. [2000] “Robust chaos generation by a perceptron,” *Europhys. Lett.* **51**, 230–236.
- Ramírez-Ávila, G. M. & Gallas, J. A. C. [2008] “Estructura del espacio de parametros para las ecuaciones del circuito de Chua,” *Revista Boliviana de Física* **14**, 1–9; Available online from <http://www.if.ufrgs.br/~jgallas>
- Ramírez-Ávila, G. M. & Gallas, J. A. C. [2009] “Quantification of regular and chaotic oscillations in Chua’s circuit with piecewise-linear and cubic terms,” in preparation.
- Rössler, O. E. [1976] “An equation for continuous chaos,” *Phys. Lett. A* **57**, 397–398.
- Rössler, O. E. [1979a] “Continuous chaos: four prototype equations,” *Ann. N Y Acad. Sci.* **316**, 376–392.
- Rössler, O. E. [1979b] “An equation for hyperchaos,” *Phys. Lett. A* **71**, 155–157.
- Segrè, E. [2007] *From Falling Bodies to Radio Waves, Classical Physicists and their Discoveries* (Dover, Mineola).
- Shilnikov, A. L. [1993] “On bifurcations of the Lorenz attractor in the Shimizu–Morioka model,” *Physica D* **62**, 338–346.
- Shilnikov, A. L., Shilnikov, L. P. & Turaev, D. V. [1993] “Normal forms and Lorenz attractors,” *Int. J. Bifurcation and Chaos* **18**, 1123–1139.
- Shilnikov, A. L. [1997] “Homoclinic phenomena in laser models,” *Comput. Math. Appl.* **34**, 245–251.
- Shilnikov, L. P., Shilnikov, A. L., Turaev, D. V. & Chua, L. O. [2001] *Methods of Qualitative Theory in Nonlinear Dynamics, Part 2* (World Scientific, Singapore).
- Vitolo, R., Glendinning, P. & Gallas, J. A. C. [2009] “Global structure of periodicity hubs in Lyapunov phase diagrams of dissipative flows,” preprint.